Chapter 11
Variation of Soil Properties in a Mollisol Profile Wall

Jenna R. Grauer-Gray and Alfred E. Hartemink

Abstract Soil variation was investigated in a Mollisol soil profile wall in south central Wisconsin, USA. The soil was classified as a fine-loamy, mixed, superactive, mesic Pachic Argiudolls. Data were collected from a 1 × 1 m soil profile wall that was divided into a 10 × 10 cm raster. The following measurements were made: volumetric moisture content, soil pH, soil organic carbon (SOC) concentration, and elemental analysis of Al, Ca, Fe, Mn, P, Si, Ti, and Zr by portable X-ray fluorescence (pXRF). Spatial variation of soil properties was analyzed and mapped. All the soil properties demonstrated horizontal variation within the soil profile. The extent of horizontal variation changed with depth. The magnitude and direction of these changes showed no general pattern, differing between the soil properties. The SOC concentration showed constant horizontal variation at all depths except 70–80 cm. The soil pH demonstrated the lowest horizontal variation in the top 30 cm of the profile. The horizontal variation of Fe concentration tended to increase with depth. Soil property depth functions showed considerable variation between vertical transects. Only the SOC concentration and the soil pH demonstrated fairly consistent responses to changes in depth. The soil showed spatial variation within soil horizons. The soil pH and the Fe concentration showed low within-horizon variation in all soil horizons. SOC concentration showed moderate within-horizon variation in the Ap1 horizon and high within-horizon variation in the Bt horizon. Overall, the Bt horizon contained the greatest spatial variation. All soil horizons contained high within-horizon variation of at least one soil property. These results have some implications for sampling pedons.

Keywords Soil variation · Soil pit wall · Soil profile · Morphometrics · Soil horizon

J.R. Grauer-Gray · A.E. Hartemink (✉)
Department of Soil Science, F.D. Hole Laboratory, University of Wisconsin—Madison, 1525 Observatory Drive, Madison, WI 53706, USA
e-mail: alfred.hartemink@wisc.edu

A.E. Hartemink and B. Minasny (eds.), *Digital Soil Morphometrics*,
Progress in Soil Science, DOI 10.1007/978-3-319-28295-4_11

11.1 Introduction

Soil scientists characterize a soil profile by dividing the profile into horizons based on soil properties observed in the field (Hartemink and Minasny 2014). These properties generally include color, texture, structure, and redoximorphic features. After soil horizon designation, one soil sample is taken from each horizon for laboratory analysis. As a result, only vertical variation of a soil profile is measured.

We used a raster approach to characterize horizontal and vertical variation of a Mollisol profile wall. A raster contains equally spaced data points (Goodchild 1992). Rasters are used to obtain, predict, and communicate spatial data in soil science. Digital soil mapping uses raster data and prediction rasters to produce rastered maps of soils and soil properties depicting the spatial variation of soils across landscapes (McBratney et al. 2003). However, few studies have used rasters to study spatial variation in a soil profile.

The objectives of our research were (i) to study horizontal and vertical variation of soil properties within a soil profile wall, (ii) to investigate within-horizon and between-horizon variation of soil properties in the soil profile, (iii) to utilize soil profile maps of soil properties to investigate patterns in the spatial variation of soil properties, (iv) to examine the homogeneity of soil horizons, and (v) to assess whether a soil profile can be accurately characterized with a one-dimensional, vertical sampling scheme.

11.2 Materials and Methods

11.2.1 Site Description

The soil was located at latitude 43° 4′ 2.88″ N and longitude 89° 32′ 8.10″ W at the University of Wisconsin-Madison West Madison Research Station in Verona, Wisconsin, USA (Fig. 11.1). The altitude of the site was 330 m.a.s.l. This area has a mean annual temperature of 7.8 °C and a mean annual precipitation of 840 mm.

The soil was formed in loess over outwash covering dolomite bedrock of Ordovician age at approximately 3.5 m depth. The vegetation was mainly grass and alfalfa. Though not cultivated at the time of this study, the site had been under agricultural use since the mid-1800s. The soil was located at the footslope landscape position and contained a buried A horizon at 59 cm depth due to the sedimentation of soil eroded from upper parts of the soilscape. An argillic horizon at 77 cm depth contained redoximorphic features.

The soil was classified as a fine-loamy, mixed, superactive, mesic Pachic Argiudolls (Troxel silt loam series). To 100 cm soil depth, the soil contained five horizons, all formed in loess (Table 11.1).

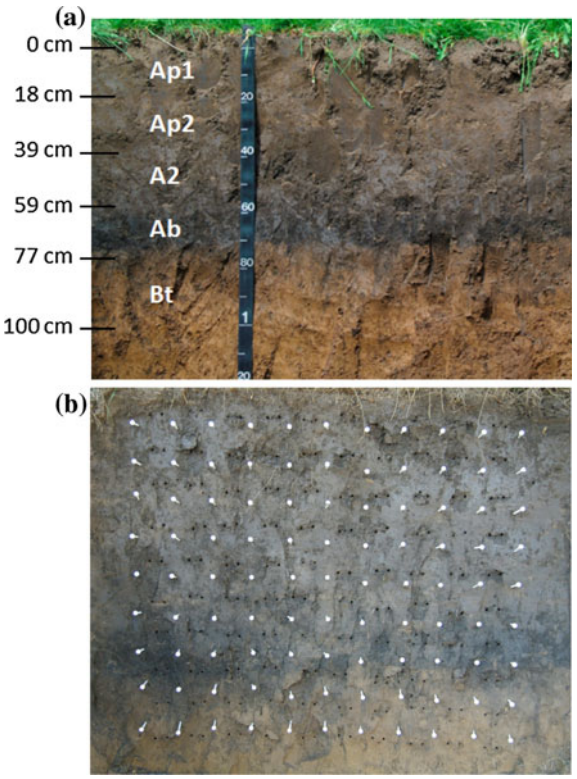

Fig. 11.1 Soil profile of a fine-loamy, mixed, superactive, mesic Pachic Argiudolls in Wisconsin, USA. **a** Soil profile with horizon designations and horizon depths indicated. **b** Soil profile rastered for field measurements and soil sampling (10 × 10 cm)

Table 11.1 Profile description of the soil (characterized to 100 cm soil depth), a fine-loamy, mixed, superactive, mesic Pachic Argiudolls located at the University of Wisconsin-Madison West Madison Research Station in Verona, Wisconsin, USA

Horizon	Depth (cm)	Dry color	Moist color	Structure	Texture	SOC (g/kg)	N (g/kg)
Ap1	0–18	Very dark brown (10YR 2/2)	Dark grayish brown (10YR 4/2)	Granular	Silt	22	2.3
Ap2	18–39	Very dark brown (10YR 2/2)	Dark grayish brown (10YR 4/2)	Platy	Silt loam	18	1.8
A2	39–59	Very dark brown (10YR 2/2)	Dark grayish brown (10YR 4/2)	Subangular blocky	Silt loam	22	2.1
Ab	59–77	Black (10YR 2/1)	Dark grayish brown (10YR 4/2)	Subangular blocky	Silt loam	27	2.3
Bt	77+	Dark yellowish brown (10YR 3/4)	Yellowish brown (10YR 5/4)	Angular blocky	Silty clay loam	8	1.6

11.2.2 Soil Sampling and Analysis

The soil profile wall was divided into a 1 × 1 m raster of 10 × 10 cm squares up to 1 m depth (Fig. 11.1). Volumetric moisture content was measured in the field in the center of each square using a time-domain reflectometer (Spectrum FieldScout TDR 300). Soil samples of approximately 200 g were collected from the center of each raster square.

Laboratory samples were air-dried. Dry and moist color measurements were taken using Munsell soil color charts. Samples were finely ground. The concentrations of Al, Ca, Fe, Mn, P, Si, Ti, and Zr were measured in the laboratory using portable X-ray fluorescence (pXRF). A Delta Professional pXRF Analyzer (Olympus Scientific Solutions Americas, Inc.) was used to scan the soil samples. The pXRF analyzer was calibrated using a 316 stainless steel calibration check reference coin. The soil organic carbon (SOC) and nitrogen concentrations were determined by LECO dry combustion. The soil pH was measured in 1:1 soil to water.

11.2.3 Data Analysis

Boxplots for each soil property were made to examine property variation within and between depth intervals and within and between soil horizons. Individual plots were created for each property. The boxplots show the median, the quartiles (excluding outliers), and the outliers at each depth or within each horizon. Property depth function plots were created by combining the soil property depth functions of the ten vertical transects of the soil profile on one plot. Depth function plots were created for every studied soil property except Ti and Zr concentrations. The midpoint of each depth interval was used as the depth value for the property measurement in that depth interval.

Soil profile maps were created for every soil property except volumetric moisture content and Ti and Zr concentrations by locating the soil property measurements of each soil sample in the center of its raster square then spatially interpolating the soil property values over the soil profile wall using block kriging and global variograms in VESPER (Minasny et al. 2005).

Statistics by depth and by horizon were calculated using the “doBy” package (Højsgaard and Halekoh 2014) within the R statistical package (R Core Team 2013). Coefficients of variation (CVs) by horizon were calculated by dividing the standard deviation by the mean.

11.3 Results

11.3.1 Variation of Soil Properties with Depth

SOC

The SOC concentration showed constant horizontal variation at all depths except at 70–80 cm soil depth (Fig. 11.2). The standard deviation was 7 g C/kg at 70–80 cm soil depth, whereas at all other depths it was below 2 g C/kg. The SOC depth functions all followed the same pattern. At 0–30 cm soil depth, the SOC concentration tended to decrease slightly with depth. At 30–70 cm soil depth, the SOC concentration tended to increase with depth. At 60–70 cm soil depth, the direction of the depth functions changed, and below 70 cm, the depth functions showed a tendency of decreasing SOC concentration with depth. The SOC depth functions all tended to have similar rates of change with depth except at 60–80 cm soil depth. At 60–80 cm soil depth, the SOC depth functions demonstrated the most dissimilarity due to varying rates of change in SOC concentration; the magnitude of the decrease in SOC concentration from 60 cm soil depth to 80 cm soil depth ranged from 0.3 g C/kg to 20 g C/kg.

pH

The lowest horizontal variation of soil pH occurred in the top 30 cm of the soil profile with standard deviations below 0.1 (Fig. 11.2). The soil pH at depths with high pH did not vary more than the soil pH at depths with low pH. The highest horizontal variation of soil pH occurred at 90–100 cm soil depth with a standard deviation exceeding 0.2. The soil pH depth functions generally followed the same pattern. The soil pH increased with depth at 0–20 and 80–100 cm soil depth. At 40–60 cm, the soil pH tended to decrease with depth. At 20–40 and 60–80 cm soil depth, the soil pH depth functions fluctuated slightly with depth and the changes did not follow a consistent pattern.

Volumetric Moisture Content

The horizontal variation of the volumetric moisture content increased with depth in the top 30 cm of the soil profile, decreased with depth until 70 cm soil depth, then stayed constant at 70–100 cm soil depth (Fig. 11.2). The highest horizontal variation of volumetric moisture content occurred at 10–40 cm soil depth with standard deviations exceeding 5 %.

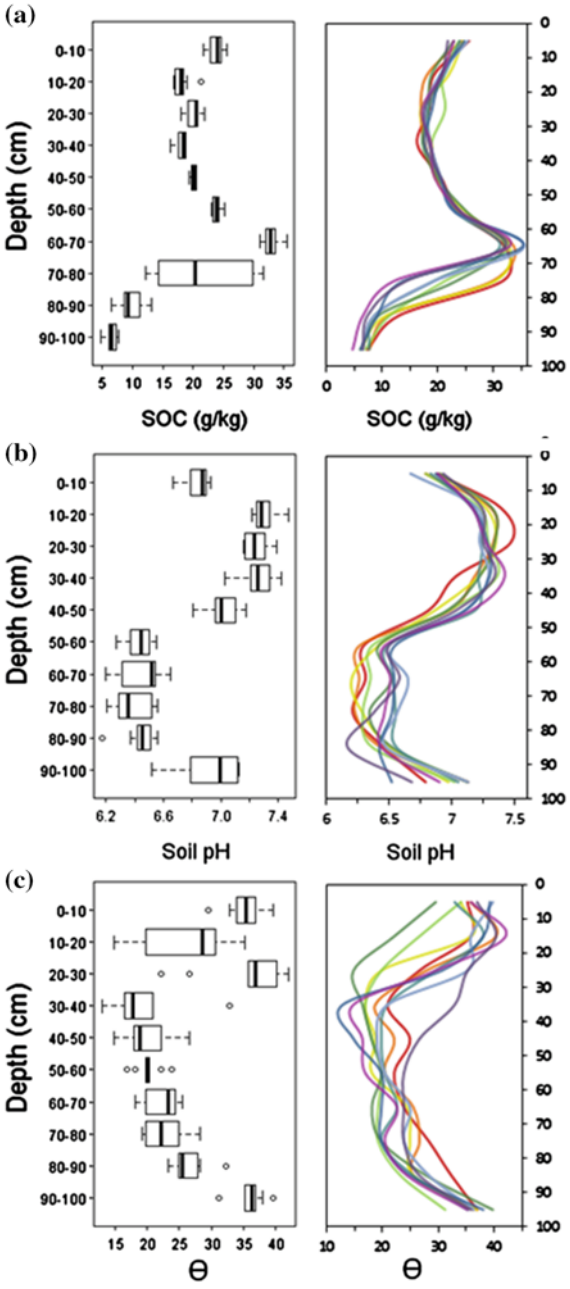

Fig. 11.2 Boxplots and depth function plots showing the horizontal and vertical variation of soil properties at each depth interval studied in a 1 × 1 m profile wall of a fine-loamy, mixed, superactive, mesic Pachic Argiudolls in Wisconsin, USA. The depth function plots contain ten individual depth functions, obtained from the ten vertical transects studied in the soil profile wall. Ten soil samples from the center of 10 × 10 cm raster squares were taken at each depth interval and from each vertical transect. **a** SOC concentration and **b** pH were obtained in the laboratory. **c** Volumetric soil moisture content (θ) was measured in the field

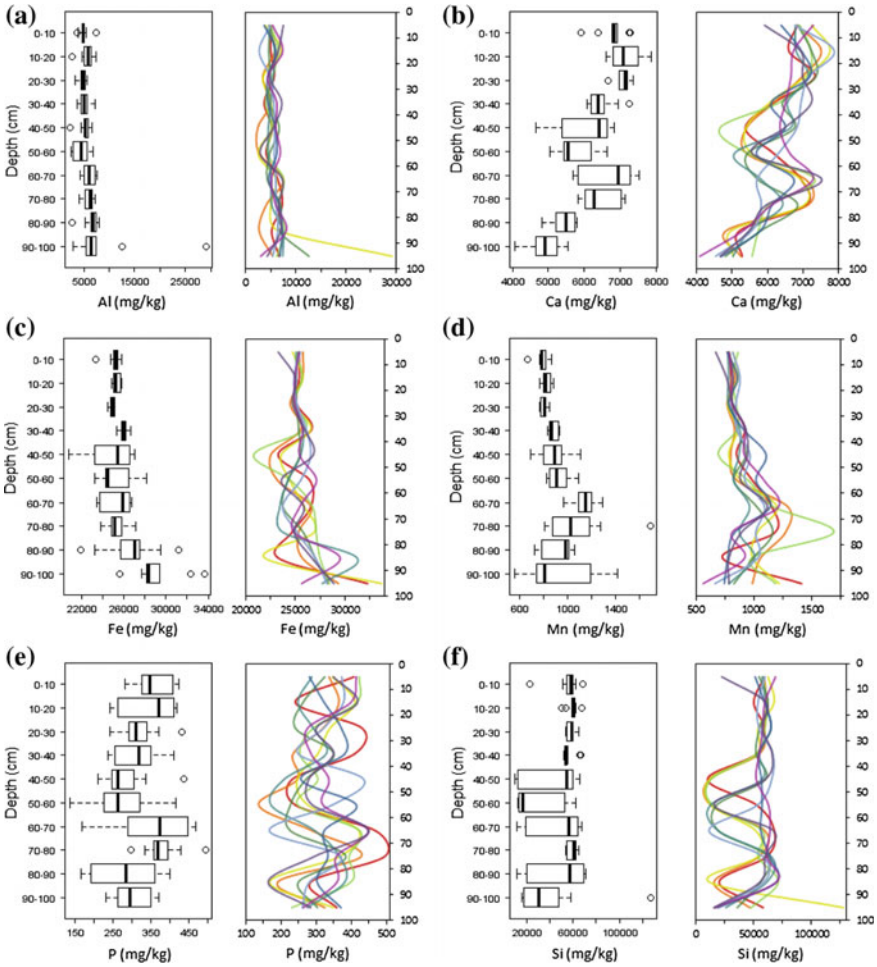

Fig. 11.3 Boxplots and depth functions showing the horizontal and vertical variation of soil properties at each depth interval studied in a 1 × 1 m profile wall of a fine-loamy, mixed, superactive, mesic Pachic Argiudolls in Wisconsin, USA. The depth function plots contain ten individual depth functions, obtained from the ten vertical transects studied in the soil profile wall. Ten soil samples from the center of 10 × 10 cm raster squares were taken at each depth interval and from each vertical transect. Elemental concentrations of **a** Al, **b** Ca, **c** Fe, **d** Mn, **e** P, and **f** Si were obtained on air-dried soil samples using pXRF

Al

The Al concentration showed relatively constant horizontal variation at all depth intervals except at 90–100 cm soil depth (Fig. 11.3). At 90–100 cm soil depth, the standard deviation was 8000 mg Al/kg; at other depths, the standard deviations were between 800 and 2000 mg Al/kg. The median Al concentrations ranged from 4000 mg Al/kg at 50–60 cm soil depth to 7000 mg Al/kg at 80–90 cm soil depth.

Ca

The horizontal variation of the Ca concentration fluctuated with depth (Fig. 11.3). The greatest horizontal variation occurred at 40–50 cm soil depth and 60–70 cm soil depth with standard deviations exceeding 700 mg Ca/kg. The lowest horizontal variation occurred at 20–30 cm soil depth with a standard deviation of 200 mg Ca/kg. The median Ca concentration ranged from 5000 mg Ca/kg at 90–100 cm soil depth to 7000 mg Ca/kg at 60–70 cm soil depth.

Fe and Mn

The horizontal variation of Fe and Mn concentrations tended to increase with depth (Fig. 11.3). The lowest horizontal variation occurred in the top 40 cm of the soil profile with standard deviations of 200–700 mg Fe/kg and of 20–50 mg Mn/kg. The horizontal variation increased below 40 cm soil depth with standard deviations of 1000–3000 mg Fe/kg and 90–300 mg Mn/kg. The median Fe and Mn concentrations stayed relatively constant with depth in the upper 60–80 cm of the soil profile with median concentrations of around 25,000 mg Fe/kg at 0–80 cm soil depth and median concentrations of around 800 mg Mn/kg at 0–60 cm soil depth. Below 80 cm soil depth, the median Fe concentration increased to 28,000 mg Fe/kg at 90–100 cm. The highest median Mn concentration occurred at 60–70 cm soil depth (1000 mg Mn/kg).

P

The horizontal variation of P concentration fluctuated with depth (Fig. 11.3). The highest horizontal variation of P concentration occurred at 60–70 cm soil depth with a standard deviation exceeding 100 mg P/kg. At other soil depths, the standard deviations ranged from 40 to 90 mg P/kg. The median P concentration ranged from 260 mg P/kg at 40–60 cm to 370 mg P/kg at 10–20 cm soil depth and 60–80 cm soil depth.

Si

The horizontal variation of Si concentration fluctuated with depth (Fig. 11.3). The lowest horizontal variation of Si concentration occurred at 0–40 cm soil depth and at 70–80 cm soil depth with standard deviations below 20,000 mg Si/kg. The highest horizontal variation occurred at 90–100 cm soil depth with a standard deviation exceeding 30,000 mg Si/kg. The median Si concentrations were relatively constant at all depths except at 50–60 cm soil depth and 90–100 cm soil depth.

Ti

The lowest horizontal variation of Ti concentration occurred in the top 40 cm of the soil profile with standard deviations below 150 mg Ti/kg. At other depths, the standard deviations ranged from 200 to 470 mg Ti/kg. The lowest median Ti concentration occurred at 50–60 cm soil depth (2900 mg Ti/kg). At other depths, the median Ti concentration remained fairly constant, ranging from 3200 to 3500 mg Ti/kg.

Zr

The highest horizontal variation of Zr concentration occurred at 70–80 cm soil depth with a standard deviation of 30 mg Zr/kg (Fig. 11.4). At other soil depths, standard deviations were below 20 mg Zr/kg. The lowest horizontal variation of Zr concentration occurred at 0–40 cm soil depth. The median Zr concentration at 0–40 cm soil depth ranged from 290 mg Zr/kg to 310 mg Zr/kg. The median Zr concentration at 40–70 cm soil depth was below 280 mg Zr/kg. The median Zr concentration at 70–100 cm soil depth exceeded 350 mg Zr/kg.

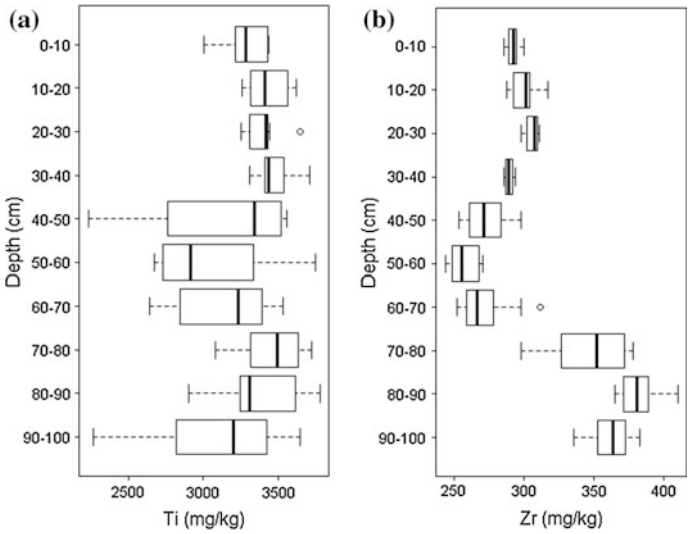

Fig. 11.4 Boxplots showing the horizontal and vertical variation of soil properties at each depth interval studied in a 1 × 1 m profile wall of a fine-loamy, mixed, superactive, mesic Pachic Argiudolls in Wisconsin, USA. Ten soil samples from the center of 10 × 10 cm raster squares were taken at each depth interval. Elemental concentrations of **a** Ti and **b** Zr were obtained on air-dried soil samples using pXRF

Table 11.2 Amount of within-horizon variation of soil properties: soil organic carbon (SOC), soil pH, volumetric moisture content (Θ), elemental concentrations of Al, Ca, Fe, Mn, P, and Si

Horizons	n	SOC	pH	Θ	Al	Ca	Fe	Mn	P	Si
Ap1	20	±	−	±	+	−	−	−	±	±
Ap2	20	−	−	+	±	−	−	−	±	−
A2	20	−	−	±	+	±	−	±	+	+
Ab	10	−	−	±	+	±	−	−	+	+
Bt	20	+	−	±	+	−	−	+	+	+

All properties except Θ were measured on air-dried soil samples in the laboratory. Amount of variation measured using coefficients of variation (CVs).
− = CV < 10 %, ± = CV 10–20 %, + = CV > 20 %

11.3.2 Variation Within Soil Horizons

The samples from 0 to 20 cm soil depth are from the Ap1 horizon, from 20 to 40 cm soil depth are from the Ap2 horizon, from 40 to 60 cm soil depth are from the A2 horizon, from 60 to 70 cm soil depth are from the Ab horizon, and from 80 to 100 cm soil depth are from the Bt horizon. The Bt horizon contained five soil properties demonstrating high (CV > 20 %) within-horizon variation (Table 11.2). The A2 and Ab horizons each contained three soil properties demonstrating high within-horizon variation. The Ap1 and Ap2 horizons contained mainly low (CV < 10 %) and moderate (CV 10–20 %) within-horizon soil property variation.

SOC

The within-horizon SOC concentrations consisted of three non-overlapping ranges (Fig. 11.5). The lowest SOC concentrations occurred in the Bt horizon (5–13 g C/kg). The Ap1, Ap2, and A2 horizons contained SOC concentrations between 16 and 26 g C/kg. The highest SOC concentrations occurred in the Ab horizon (31–35 g C/kg). The lowest within-horizon variation of SOC occurred in the Ap2 and Ab horizons (CV < 6 %). The Ap1 and A2 horizons had CVs of about 10 %. The highest within-horizon variation of SOC concentration occurred in the Bt horizon (CV 30 %).

pH

The highest soil pH occurred in the Ap1 and Ap2 horizons (Fig. 11.5). The pH showed low within-horizon variation in all the horizons with CVs lower than 5 %. The lowest within-horizon variation occurred in the Ap2 and Ab horizons.

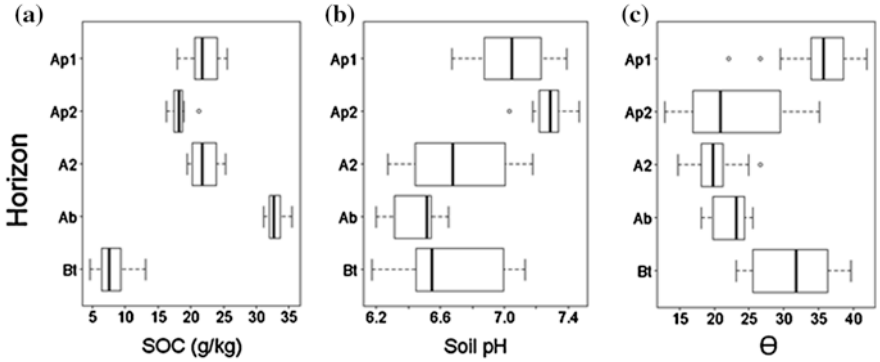

Fig. 11.5 Boxplots showing within- and between-horizon variation of soil properties in the five horizons studied in a 1 × 1 m profile wall of a fine-loamy, mixed, superactive, mesic Pachic Argiudolls in Wisconsin, USA. Soil samples were collected from the center of 10 × 10 cm raster squares and **a** SOC concentration and **b** soil pH were measured in the laboratory. **c** Volumetric soil moisture content (θ) was measured in the field in the center of 10 × 10 cm raster squares

Volumetric Moisture Content

Volumetric moisture content demonstrated moderate to high within-horizon variation with CVs ranging from 11 % to 31 % (Fig. 11.5).

Al

The lowest median Al concentrations occurred in the Ap1, Ap2, and A2 horizons with median concentrations of 5000 mg Al/kg (Fig. 11.6). The Ab horizon had a median concentration of 6000 mg Al/kg, and the Bt horizon had a median Al concentration of 7000 mg Al/kg. The highest within-horizon variation of Al concentration occurred in the Bt horizon (CV > 70 %). The other soil horizons contained moderate to high within-horizon variation of Al concentration with CVs below 30 %.

Ca

The lowest median Ca concentrations occurred in the Ab and Bt horizons with median concentrations below 6000 mg Ca/kg (Fig. 11.6). The Ap1, Ap2, and Ab horizons had median Ca concentrations of 7000 mg Ca/kg. The Ap1 and Ap2 horizons had the lowest within-horizon variation of Ca with CVs lower than 7 %. The A2, Ab, and Bt horizons had CVs around 10 %.

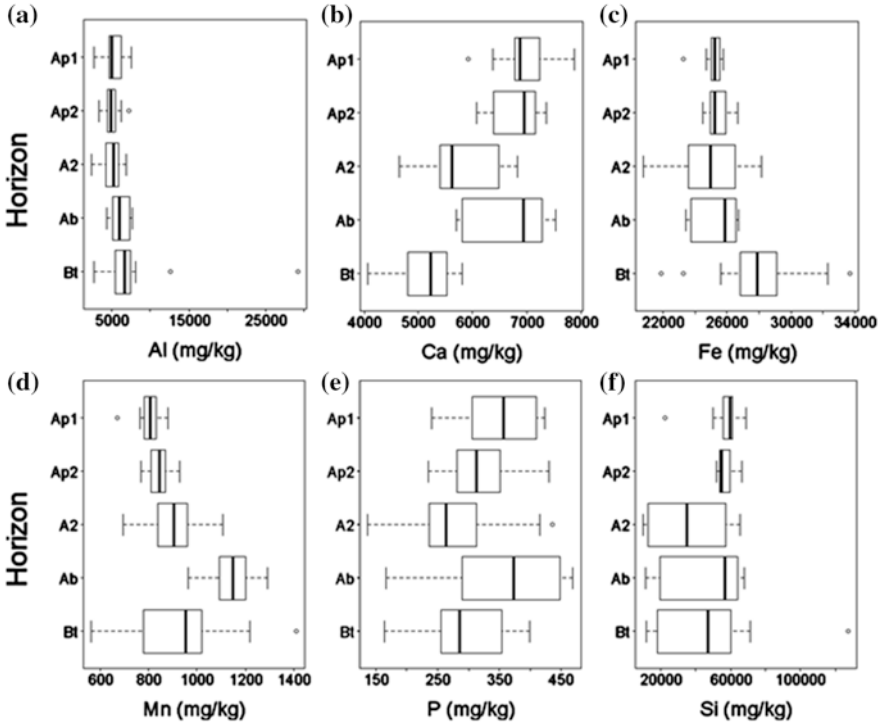

Fig. 11.6 Boxplots showing within- and between-horizon variation of soil properties in the five horizons studied in a 1 × 1 m profile wall of a fine-loamy, mixed, superactive, mesic Pachic Argiudolls in Wisconsin, USA. Soil samples were collected from the center of 10 × 10 cm raster squares and the following elemental concentrations were measured in the laboratory: **a** Al, **b** Ca, **c** Fe, **d** Mn, **e** P, **f** Si

Fe

The highest Fe concentration occurred in the Bt horizon with a median concentration of 28,000 mg Fe/kg (Fig. 11.6). The other horizons contained median concentrations of about 25,000 mg Fe/kg. The lowest within-horizon variation of Fe concentration occurred in the Ap1 and Ap2 horizons (CV < 3 %). The highest within-horizon variation of Fe concentration occurred in the Bt horizon (CV 10 %).

Mn

The highest median Mn concentration occurred in the Ab horizon with a median concentration exceeding 1000 mg Mn/kg (Fig. 11.6). The Ap1, Ap2, A2, and Bt horizons contained median concentrations of 800–1000 mg Mn/kg. The Ap1 and Ap2 horizons had the lowest within-horizon variation of Mn concentration

(CV < 6 %). The Bt horizon had the highest within-horizon variation of Mn concentration with a CV exceeding 20 %.

P

The lowest P concentration occurred in the A2 horizon with a median concentration of 260 mg P/kg (Fig. 11.6). The highest median P concentrations occurred in the Ap1 and Ab horizons with median concentrations exceeding 350 mg P/kg. The lowest within-horizon variation of P concentration occurred in the Ap1 and Ap2 horizons. The highest within-horizon variation of P concentration occurred in the Ab horizon (CV 30 %).

Si

The lowest median Si concentration occurred in the A2 horizon with a median concentration of 35,000 mg Si/kg (Fig. 11.6). The Bt horizon had a median concentration of 47,000 mg Si/kg. The highest median Si concentrations occurred in the Ap1, Ap2, and Ab horizons with median concentrations between 55,000 and 60,000 mg Si/kg. The lowest within-horizon variation of Si concentration occurred in the Ap2 horizon (CV 8 %). High within-horizon variation of Si concentration occurred in the Ab horizon (CV 50 %) and the highest within-horizon variation of Si concentration occurred in the A2 and Bt horizons with CVs exceeding 60 %.

11.3.3 Variation Between Soil Horizons

Between the Ap1 and the Ap2 horizons, three soil properties demonstrated little (ΔCV 1–5 %) change in within-horizon variation and one soil property demonstrated medium (ΔCV 5–10 %) change in within-horizon variation (Table 11.3). One soil property demonstrated large (ΔCV 10–20 %) change in within-horizon variation between the Ap1 and Ap2 horizons, between the Ap2 and the A2 horizons and between the A2 and the Ab horizons. One soil property demonstrated very large (ΔCV > 20 %) change in within-horizon variation between the Ap2 and the A2 horizons. Between the Ab and the Bt horizons, four soil properties demonstrated large or very large changes of within-horizon variation.

Within-horizon variation of SOC concentration and Al concentration showed little change between all adjacent horizons except the Ab and Bt horizons. Between the Ab and the Bt horizons, the within-horizon variation of SOC and Al concentrations demonstrated very large changes. The within-horizon variation of Si concentration and Mn concentration demonstrated large changes between the Ab and the Bt horizons.

Table 11.3 Change in within-horizon variation of soil properties between adjacent horizons

Horizons	SOC	pH	Θ	Al	Ca	Fe	Mn	P	Si
Ap1 → Ap2	↓	↓	↑↑↑	↓	≈	≈	≈	≈	↓↓
Ap2 → A2	↑	↑	↓↓↓	↑↑	↑	↑	↑↑	↑↑	↑↑↑↑
A2 → Ab	↓	↓	↓	↓	≈	↓	↓	↑	↓↓↓
Ab → Bt	↑↑↑↑	↑	↑↑	↑↑↑↑	↓	↑	↑↑↑	↓↓	↑↑↑

≈: change of <1 %, ↑/↓: increase/decrease of 1–5 %, ↑↑/↓↓: increase/decrease of 5–10 %, ↑↑↑/↓↓↓: increase/decrease of 10–20 %, and ↑↑↑↑: increase of >20 %

11.3.4 Soil Profile Maps of SOC Concentration and Soil pH

The soil profile map of SOC concentration divided the profile into four layers: a layer of medium SOC concentration between 0 and about 57 cm soil depth, a layer of high SOC concentration between about 57 and 72 cm soil depth, another layer of medium SOC concentration between about 72 and 81 cm soil depth, and a layer of low SOC concentration below 81 cm soil depth (Fig. 11.7). A nearly level horizontal boundary occurred between the first and the second layers of the soil profile map. Wavy boundaries occurred between the second and third layers, and the third and fourth layers of the soil profile map.

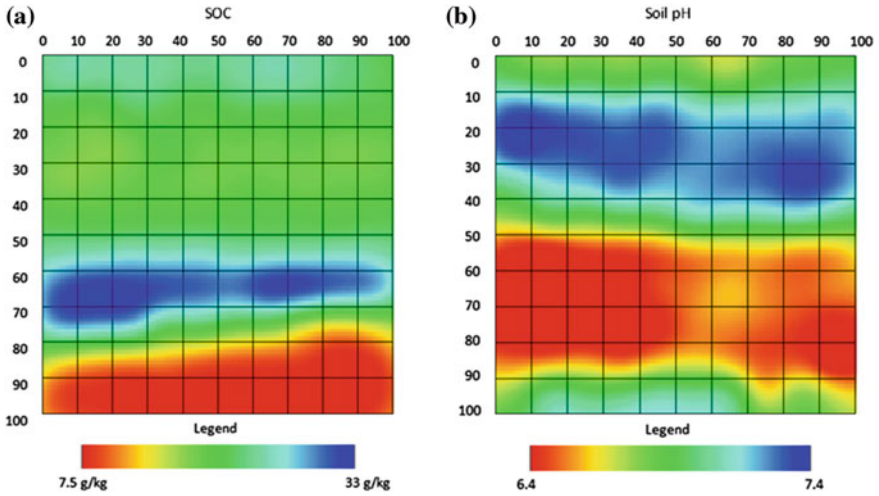

Fig. 11.7 Soil profile maps showing spatial variation of a mixed, superactive, mesic Pachic Argiudolls in Wisconsin, USA. Soil samples (n = 100) sampled from the center of 10 × 10 cm raster squares. **a** SOC concentration and **b** soil pH were obtained in the laboratory. Soil profile maps were created for each soil property by locating the measured values of each soil sample in the center of its column and depth interval then spatially interpolating the soil property values over the soil profile wall using block kriging and global variograms in Vesper 1.6 (Australian Center for Precision Agriculture)

The soil profile map of soil pH consisted mainly of two layers: a layer of high soil pH at about 10–40 cm soil depth and a layer of low soil pH at 50–90 cm soil depth (Fig. 11.7). Thin layers of medium soil pH occurred at about 0–10 cm, 40–50 cm, and 90–100 cm soil depth. An area of medium-high soil pH occurred at about 90–100 cm soil depth. All of the layers had wavy boundaries.

11.3.5 Soil Profile Maps of Elemental Concentrations

Al

The soil profile map of Al concentration showed a pattern of increasing Al concentration with depth in the horizontal range of 0–80 cm (Fig. 11.8). At 80–100 cm

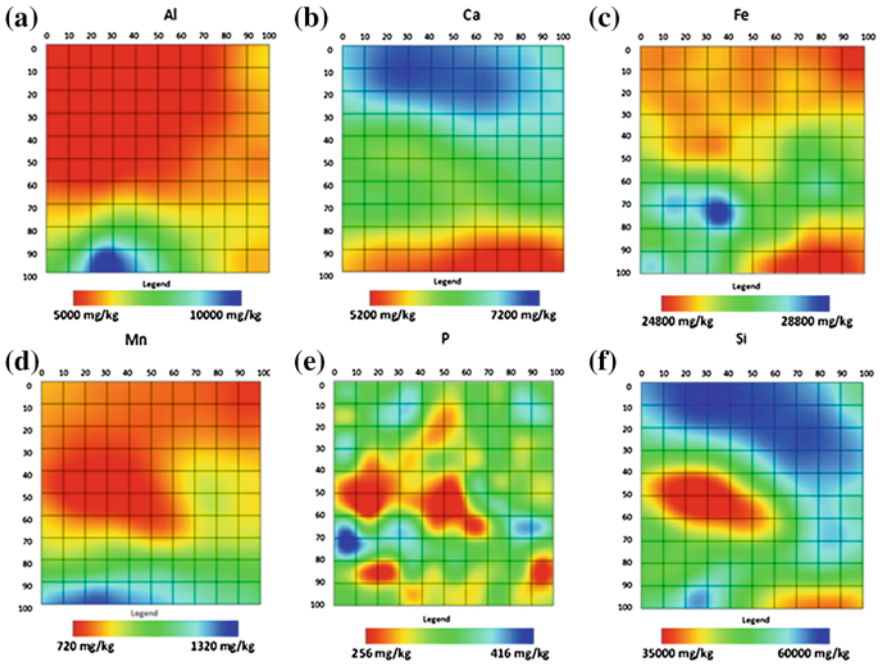

Fig. 11.8 Soil profile maps showing spatial variation of a mixed, superactive, mesic Pachic Argiudolls in Wisconsin, USA. Soil samples (n = 100) from the center of 10 × 10 cm raster squares. Elemental concentrations of **a** Al, **b** Ca, **c** Fe, **d** Mn, **e** P, and **f** Si were obtained in the laboratory using pXRF. Soil profile maps were created for each soil property by locating the measured values of each soil sample in the center of its column and depth interval then spatially interpolating the soil property values over the soil profile wall using block kriging and global variograms in Vesper 1.6 (Australian Center for Precision Agriculture)

horizontally, the Al concentration remained relatively constant with depth. The increase in Al concentration with depth occurred irregularly. The greatest increase in Al concentration with depth occurred at 20–40 cm horizontally.

Ca

The soil profile map of Ca concentration showed a pattern of decreasing Ca concentration with depth (Fig. 11.8). The soil profile map of Ca concentration had three main layers: a top layer of high Ca concentration, a middle layer of medium Ca concentration, and a bottom layer of low Ca concentration. The top layer had an irregular lower boundary, beginning at 20–30 cm soil depth at 0–10 cm horizontally then decreasing in depth and becoming more diffuse. The middle layer had a less irregular but still wavy lower boundary. Also, a few areas of increasing Ca concentration with depth occurred: at 70–100 cm horizontally at 0–20 cm soil depth, at 0–40 cm horizontally at 40–60 cm soil depth, and at 50–60 cm horizontally at 50–80 cm soil depth.

Fe

The soil profile map of Fe concentration had two large areas: an area of low Fe concentration in the upper 30–50 cm of the soil profile and an area of medium concentration located between 30 cm and 100 cm soil depth (Fig. 11.8). Small areas of high Fe concentration occurred between 60 cm and 80 cm soil depth. An area of low Fe concentration occurred below 70 cm soil depth at 50–100 cm horizontally.

Mn

The soil profile map of Mn concentration contained three main layers: a layer of low Mn concentration at about 0–70 cm soil depth, a layer of medium Mn concentration at about 70–100 cm soil depth, and a layer of high Mn concentration at about 90–100 cm soil depth (Fig. 11.8). The boundary between the top and the middle layers occurred at 60–80 cm soil depth at 0–60 cm horizontally and at 90–100 cm horizontally. At 60–90 cm horizontally, the layer of medium Mn concentration had a tongue-shaped extension, which stretched up to about 40 cm soil depth. At 20–70 cm horizontally, the boundary between the middle and the bottom layers occurred at 80–90 cm depth, but the boundary occurred at 90–100 cm depth elsewhere in the profile.

P

The soil profile map of P concentration showed an apparently random distribution of P content in the profile (Fig. 11.8). The map had scattered areas of high, medium, and low P concentration.

Si

The soil profile map of Si concentration showed a pattern of decreasing Si concentration with depth in the top 70 cm of the profile (Fig. 11.8). A region of high Si concentration occurred in the top 0–50 cm of the soil profile. Small areas of medium-high to high Si concentration occurred below 50 cm soil depth. Areas of low Si concentration occurred between 30 and 70 cm soil depth and below 90 cm soil depth.

11.4 Discussion

11.4.1 Application of Digital Soil Morphometrics

In this study, we applied digital soil morphometrics to quantitatively measure soil profile properties, to create continuous depth functions, and to investigate spatial variation of soil properties in a soil profile wall (Hartemink and Minasny 2014). The technique of rastering allowed us to study horizontal and vertical variation at fixed depth increments and to create soil property depth functions and soil profile maps showing the variation of soil properties. We used the pXRF analyzer and the TDR to obtain rapid measurements of elemental concentrations and volumetric soil moisture content. A similar approach was used by Adhikari et al. (2016) who applied soil profile wall rastering, TDR, pXRF, and spatial interpolation to study soil profile properties. In a study of soil hydrology, Netto et al. (1999) used a grid method to study horizontal and vertical variation, sampling every 10 cm horizontally over a 1.2 m distance, and sampling nine depth ranges (5–6 cm deep) between 0 and 1.05 m soil depth. Schwen et al. (2014) used a three-dimensional raster sampling scheme to study solute movement and soil physical properties in soil pedons, sampling every 10 cm in each dimension.

Digital soil morphometrics enables investigation of variation within soil profiles, variation that would be overlooked when using traditional methods. Buddenbaum and Steffens (2012) imaged an undisturbed soil profile in the laboratory using high-resolution vis-NIR (400–1000 nm) spectroscopy. They detected spatial variation within the profile using the resulting images. Steffens et al. (2014) used the same technique to identify SOM fractions in a visually uniform organic soil profile. Roudier et al. (2016) collected spectroscopic (350–2500 nm) images of three soil

profiles in the laboratory. Using principal component analysis and segmentation, they created false color images showing horizontal variation within the profile. They also found vertical variation within horizons and the presence of a possible horizon boundary not detected when horizonating the soil profile using traditional characterization tools and techniques.

11.4.2 Horizontal Variation of Soil Properties

All studied soil properties demonstrated horizontal variation within the soil profile. The extent of horizontal variation changed with depth. The magnitude and direction of these changes showed no general pattern, differing between soil properties. In their study of a Psamment soil profile, Adhikari et al. (2016) observed considerable horizontal variation and soil property-dependent patterns of variation. Netto et al. (1999) observed considerable horizontal variation of volumetric soil moisture content in coarse-textured soil profiles.

Cultivation and Bioturbation

The lowest horizontal variation of soil pH occurred in the top 30 cm of the soil profile, and the lowest horizontal variation of Al, Fe, Mn, Si, Ti, and Zr concentrations occurred in the top 40 cm of the soil profile. The Al, Fe, Mn, Si, Ti, and Zr concentrations also demonstrated low vertical variation between 0 and 40 cm soil depth. This 0–40 cm depth range corresponded to the location of the Ap1 and Ap2 horizons, the horizons that have undergone haploidization due to plowing and sedimentation. Other studies have found low spatial variation in the top 30–40 cm of soil profiles with a history of cultivation. Adhikari et al. (2016) noted that the lowest spatial variability occurred in the top 40 cm of their soil profile. Franklin et al. (2003) found no difference between the concentrations of Al, Fe, Mn, Zr, and Ti and twenty other elements between the 0–15 cm and the 15–30 cm soil depth ranges in 27 soil profiles with a history of cultivation.

Haploidization due to cultivation of the top 40 cm cannot completely explain the spatial variation of soil pH at the 0–40 cm soil depth. The soil pH demonstrated vertical variation at 0–40 cm soil depth and horizontal variation at 30–40 cm soil depth. Soil haploidization due to bioturbation may have contributed to low horizontal variation of pH. Bioturbation can reduce variation in soil and tends to occur most intensely near the soil surface (Hole 1981; Wilkinson et al. 2009).

SOC

The SOC concentration increased with depth at 30–70 cm soil depth, possibly due to a decreasing rate of decomposition of soil organic matter (SOM). With increasing

soil depth, SOM decomposition rates tend to decrease (Gregorich et al. 1998; Helgason et al. 2014). The horizontal variation of SOC concentration was more or less constant at all depths except 70–80 cm soil depth. The higher horizontal variation of SOC at 70–80 cm resulted from the presence of the boundary between the Ab horizon and the subsoil (Bt horizon). This boundary effect seems to increase spatial variation of SOC concentration. Mapping a soil profile using high-resolution vis-NIR spectroscopy, Steffens and Buddenbaum (2013) found larger spatial variability in the transition zone between the topsoil (A) and the subsoil (E) horizons of their profile than within the individual horizons.

Volumetric Moisture Content

The volumetric moisture content demonstrated horizontal variation with standard deviations between 2 and 8 %. Netto et al. (1999) found moderate horizontal variation (CV 5–20 %) in a coarse-textured soil profile and non-significant correlation of the volumetric moisture content horizontally.

Al and Si

The Al and Si concentrations demonstrated increasing horizontal variation with depth at 70–100 cm soil depth, the depth range containing the Bt horizon. The increasing variation probably reflects increasingly irregular distribution of illuviated aluminosilicate clays with depth. The low spatial variation of Al and Si concentrations in the top 40 cm of the soil profile may result from an even distribution of aluminosilicate clay. At 40–70 cm soil depth, Al concentration showed low spatial variation, but Si concentration showed high spatial variation. A factor other than distribution of aluminosilicate clays is needed to explain the variation of Al and Si concentrations at 40–70 cm soil depth.

11.4.3 Utility of Soil Depth Functions

Soil profile studies have used soil depth functions to help characterize soil profiles and identify soil processes (e.g. Gaikawad and Hole 1965; Eswaran and Bin 1978). Minasny et al. (2016) used soil depth functions to derive soil horizon boundaries. However, the soil property depth functions in our soil profile changed between vertical transects. Sampling the vertical transect at 0–10 cm horizontally resulted in different depth functions for most soil properties than sampling the adjacent vertical transect at 10–20 cm horizontally or sampling the vertical transect at 90–100 cm horizontally. Only the depth functions of SOC concentration and soil pH maintained relatively constant shapes across the ten vertical transects.

11.4.4 Ti and Zr

The Ti concentration remained relatively constant throughout the soil profile. The Zr concentrations divided the soil profile into three zones: a region of medium Zr concentration at 0–40 cm soil depth, a region of low Zr concentration at 40–70 cm soil depth, and a region of high Zr concentration at 70–100 cm soil depth. Since Zr is relatively immobile in the soil, changes in Zr concentrations may reflect differences in parent material (Schaetzl 1998). The top 100 cm of this soil profile formed in loess, but loess from different depositional events may differ in chemical composition (Muhs and Bettis 2000). The decrease in Zr concentration at 40 cm soil depth may result from the loess parent material having a different chemical composition as compared to the 40–70 cm soil depth. The 40–70 cm soil depth contained the majority of the buried A horizon with approximately 20 cm of deposited material above it. This 20 cm of deposited material may have been transported from nearby areas with the same type of loess parent material as the buried A horizon. The increase in Zr concentration at 70–80 cm soil depth may result from a different loess parent material.

11.4.5 Variation Within and Between Soil Horizons

We found that soil properties show considerable horizontal and within-horizon variation, variation that cannot be detected using one-dimensional vertical sampling schemes. We found moderate to very high spatial variation of at least three soil properties within all horizons studied. This high within-horizon variation implies that horizon characterization using one sample per horizon does not always estimate the average value of a soil property within the horizon.

Stolt et al. (1993) found considerable variation of soil properties within soil horizons. They used four soil samples from the corners of 1 × 1 m lateral horizon cross sections. They found an average CV of 10 % and a maximum CV of 40 % for extractable Al and Fe within Bt horizons. They suggested taking multiple samples from a soil horizon to increase the accuracy of soil profile characterization.

SOC, Al, and Si

In our soil profile, the SOC, Al, and Si concentrations demonstrated high within-horizon variation in the Bt horizon. The high variation of Al and Si concentrations may result from the uneven distribution of illuviated aluminosilicate clays. SOM may have been transported into the Bt horizon in conjunction with clay, contributing to high variation of SOC in the Bt horizon. SOC can be transported within a soil profile as clay-humus chelates (Miedema et al. 1999). Another factor that could have contributed to the high variation of SOC may be spatially localized sources of SOM, for example, plant roots and fungal hyphae.

The high to very high increase in within-horizon variation of Al and Si concentrations between the Ab and the Bt horizons may occur because of the lower concentration and possibly more even distribution of clay and of clay-associated SOM in the Ab horizon. This may also partly explain the change in within-horizon variation of SOC concentration. However, most of the SOC in the Ab horizon resulted from the horizon being a former surface horizon. The low within-horizon variation of SOC concentration in the Ab horizon may result from bioturbation that occurred when the horizon was at the soil surface.

The increase in SOC concentration between the A2 and the Ab horizons probably results from the preservation of SOC in the Ab horizon. As the surface horizon of a Mollisol, the Ab horizon would have contained high SOC concentration, and the burial of the horizon probably resulted in very low SOM decomposition rates, thus preserving SOC. SOM decomposition rates tend to decrease with increasing depth from the soil surface (Gregorich et al. 1998; Helgason et al. 2014).

A decrease in the SOM decomposition rates with depth may have contributed to the increase in SOC concentration between the Ap2 horizon and the A2 horizon. Increased decomposition rates in the Ap2 horizon due to tillage may also have contributed to the increase in SOC concentration between the Ap2 horizon and the A2 horizon. Tillage generally increases the rate of SOM decomposition, thus reducing SOC concentration (Martel and Paul 1974; Tisdall and Oades 1982; Puget and Lal 2005).

Fe and Mn

The Fe and Mn concentrations demonstrated the highest within-horizon variation in the Bt horizon. Much of this variation resulted from the occasional saturation of this horizon, as evidenced by the presence of redoximorphic features. Mobility of Fe and Mn tends to increase with soil saturation due to decreased oxygen concentration, reducing Fe and Mn concentrations in parts of the soil horizon (Christensen et al. 1951; Callebaut et al. 1982; Patrick and Jugsujinda 1992). Conversely, Fe and Mn precipitate when the horizon drains and reoxidizes, thus increasing Fe and Mn concentrations in parts of the soil horizon (Gotoh and Patrick 1972, 1974; Atta et al. 1996). The low density of redoximorphic features in the Bt horizon implies that the soil horizon primarily experienced short-term saturation. The predominant short-term saturation explains the high within-horizon variation of Mn and the low within-horizon variation of Fe in the Bt horizon. Mn becomes mobile in less reducing conditions than Fe and thus is transported in periods of saturation too short to produce the degree of reduction needed to transport Fe (Olomu et al. 1973; Patrick and Jugsujinda 1992).

11.4.6 Interpretations of Soil Profile Maps

SOC

The soil profile map of SOC concentration confirmed the presence of three main horizons: an A horizon formed in material deposited by soil erosion, the buried A horizon, and the Bt horizon. The third layer we designated as a transition zone between the Ab and the Bt horizons because the Ab/Bt horizon boundary occurred in this layer and because based on the high horizontal variation of SOC concentration at 70–80 cm depth, the sampling occurred around the Ab/Bt boundary. The wavy boundaries of this transition zone imply a wavy Ab/Bt boundary.

pH and Ca

The soil profile map of soil pH divided the soil profile differently than the soil profile map of SOC concentration. The high soil pH of the second layer likely resulted from liming and incorporation of lime by tillage, and the top layer probably had a similar soil pH when the soil was regularly limed and plowed. The medium soil pH of the top layer likely resulted from a decrease in soil pH due to acidification processes such as additions of acids to the soil by rainfall and production of organic acids by plant roots and microbes (Gerretsen 1948; Jones and Darrah 1994). Together these top two layers corresponded to the A horizons that showed evidence of cultivation, the Ap1 and Ap2 soil horizons. The bottom layers of the soil profile map did not correspond with soil horizons. The thin third layer is a transition zone between the second and the fourth layers, the two main layers of the soil profile map. The fourth layer, a layer of low pH, probably resulted from this soil being below the region of lime incorporation. The increase in pH at around 85 cm soil depth may have resulted from the upward movement of water through underlying calcareous material, although the lowest Ca concentrations in the soil profile also occurred in this region.

The soil profile map of Ca concentration divided soil profile differently than the soil profile maps of SOC concentration and soil pH. The high Ca concentration in the top layer probably resulted from the application and incorporation of lime. The high horizontal variation of Ca concentration in the top layer may result from spatially differing levels of Ca removal by plant uptake and leaching. The second layer of the profile map may contain the Ca concentration of the soil with minimal additions through liming. However, Ca leached from above may have raised the Ca concentration in this layer. This could help explain the decrease in Ca concentration below the second layer. The lower layer of the profile map occurred within the Bt horizon, which had a finer texture than the horizons above. This change in texture would slow downward movement of water, reducing the amount of Ca received through leaching. However, part of the Bt horizon was located within the middle layer. Preferential flow increasing the amount of Ca received through leaching or reducing the amount of Ca removed by leaching may explain this discrepancy.

11.5 Conclusions

A raster sampling scheme can be used to examine horizontal and vertical variation within a soil profile, as well as within- and between-horizon variation of soil properties. However, this sampling scheme can also result in sampling at horizon boundaries, thus obtaining samples containing soil from two different horizons.

Profile maps of soil properties can be used to detect patterns in spatial distribution of soil properties. Distribution of SOC concentration has potential for establishing the location of horizon boundaries. Distribution of Ca concentration has potential for establishing the location of boundaries between an A horizon and a subsoil horizon of Mollisol.

The studied soil properties demonstrated horizontal variation within the distance of 1 m. SOC concentration and pH demonstrated fairly consistent responses to changes in depth within the distance of 1 m. The other soil properties demonstrated different responses to changes in depth depending on the vertical raster column studied. To accurately characterize soil property changes with depth, depth functions may require several vertical sampling transects of the soil profile.

Within-horizon variation occurred in all the soil horizons. The magnitude of the variation depended on the soil horizon and the soil property. Overall, the within-horizon variation of the soil properties studied was highest in the Bt horizon and lowest in the Ap2 horizon. The soil pH and the Fe concentration exhibited low within-horizon variation. The Al concentration and the volumetric moisture content were the only soil properties which did not demonstrate low within-horizon variation in any horizon. The volumetric moisture content and the SOC, Al, Mn, P, and Si concentrations each exhibited high within-horizon variation in at least one horizon. The lowest within-horizon variation of Ca, Mn, and Si concentrations occurred in the cultivated horizons (Ap1 and Ap2) of this profile. The surface horizon (Ap1) contained high within-horizon variation of Al concentration and moderate within-horizon variation of volumetric moisture content and SOC, P, and Si concentrations. Below the surface horizon, the within-horizon variation tended to increase with depth.

Acknowledgements This research was supported by a Hatch project of the National Institute of Food and Agriculture, United States Department of Agriculture, accession number 1003083. We wish to thank Kabindra Adhikari, Benito Bonfatti, Corey Breseman, Luis Reyes-Rojas, and Jenifer Yost for their support and their assistance in obtaining the data used in this study.

References

Adhikari K, Hartemink AE, Minasny B (2016) Mapping a profile wall of a typic udipsamments from the Central Sands, WI, USA. In: Hartemink AE, Minasny B (eds) Digital soil morphometrics. Springer, Dordrecht

Atta SK, Mohammed SA, VanCleemput O, Zayed A (1996) Transformations of iron and manganese under controlled E(h), E(h)-pH conditions and addition of organic matter. Soil Technol 9:223–237. doi:10.1016/s0933-3630(96)00013-x

Buddenbaum H, Steffens M (2012) The effects of spectral pretreatments on chemometric analyses of soil profiles using laboratory imaging spectroscopy. Appl Environ Soil Sci 2012:1–12. doi:10.1155/2012/274903

Callebaut F, Gabriels D, Minjauw W, De Boodt M (1982) Redox potential, oxygen diffusion rate, and soil gas composition in relation to water table level in two soils. Soil Sci 134:149–156. doi:10.1097/00010694-198209000-00001

Christensen PD, Toth SJ, Bear FE (1951) The status of soil manganese as influenced by moisture, organic matter, and pH. Soil Sci Soc Am Proc 1950:279–282. doi:10.2136/sssaj1951.036159950015000C0064x

Eswaran H, Bin WC (1978) Study of a deep weathering profile on granite in peninsular Malaysia. 1. Physicochemical and micro-morphological properties. Soil Sci Soc Am J 42:144–149. doi:10.2136/sssaj1978.03615995004200010033x

Franklin R, Duis L, Smith B, Brown R, Toler J (2003) Elemental concentrations in soils of South Carolina. Soil Sci 168:280–291. doi:10.1097/00010694-200304000-00005|10.1097/01.ss.0000064891.94869.el

Gaikawad ST, Hole FD (1965) Characteristics and genesis of a gravelly brunizemic regosol. Soil Sci Soc Am Proc 29:725–728. doi:10.2136/sssaj1965.03615995002900060035x

Gerretsen FC (1948) The influence of microorganisms on the phosphate intake by the plant. Plant Soil 1:51–81. doi:10.1007/bf02080606

Goodchild M (1992) Geographical data modeling. Comput Geosci 18:401–408. doi:10.1016/0098-3004(92)90069-4

Gotoh S, Patrick WH (1972) Transformation of manganese in a waterlogged soil as affected by redox potential and pH. Soil Sci Soc Am Proc 36:738–742. doi:10.2136/sssaj1972.03615995003600050018x

Gotoh S, Patrick WH (1974) Transformation of iron in a waterlogged soil as influenced by redox potential and pH. Soil Sci Soc Am J 38:66–71. doi:10.2136/sssaj1974.03615995003800010024x

Gregorich EG, Greer KJ, Anderson DW, Liang BC (1998) Carbon distribution and losses: erosion and deposition effects. Soil Tillage Res 47:291–302. doi:10.1016/s0167-1987(98)00117-2

Hartemink AE, Minasny B (2014) Towards digital soil morphometrics. Geoderma 230:305–317. doi:10.1016/j.geoderma.2014.03.008

Helgason BL, Konschuh HJ, Bedard-Haughn A, VandenBygaart AJ (2014) Microbial distribution in an eroded landscape: buried A horizons support abundant and unique communities. Agric Ecosyst Environ 196:94–102. doi:10.1016/j.agee.2014.06.029

Højsgaard, S, Halekoh U, Robison-Cox J, Wright K, Leidi AA et al (2014) doBy: Groupwise statistics, LSmeans, linear contrasts, utilities. R package version 4.5–13. Url:http://CRAN.R-project.org/package=doBy

Hole FD (1981) Effects of animals on soil. Geoderma 25:75–112. doi:10.1016/0016-7061(81)90008-2

Jones DL, Darrah PR (1994) Role of root derived organic acids in the mobilization of nutrients from the rhizosphere. Plant Soil 166:247–257. doi:10.1007/bf00008338

Martel YA, Paul EA (1974) Effects of cultivation on the organic matter of grassland soils as determined by fractionation and radiocarbon dating. Can J Soil Sci 54:419–426. doi:10.4141/cjss74-056

McBratney AB, Santos M, Minasny B (2003) On digital soil mapping. Geoderma 117:3–52. doi:10.1016/S0016-7061(03)00223-4

Miedema R, Koulechova IN, Gerasimova MI (1999) Soil formation in Greyzems in Moscow district: micromorphology, chemistry, clay mineralogy and particle size distribution. Catena 34:315–347. doi:10.1016/s0341-8162(98)00105-2

Minasny B, McBratney AB, Whelan BM (2005) VESPER version 1.6. Australian Centre for Precision Agriculture, McMillan Building A05, The University of Sydney, NSW 2006. url: http://www.usyd.edu.au/su/agric/acpa

Muhs DR, Bettis EA (2000) Geochemical variations in Peoria Loess of western Iowa indicate paleowinds of midcontinental North America during last glaciation. Quatern Res 53:49–61. doi:10.1006/qres.1999.2090

Minasny B, Stockmann U, Hartemink AE, McBratney AB (2016) Measuring and modelling soil depth functions. In: Hartemink AE, Minasny B (eds) Digital soil morphometrics. Springer, Dordrecht

Netto AM, Pieritz RA, Gaudet JP (1999) Field study on the local variability of soil water content and solute concentration. J Hydrol 215:23–37. doi:10.1016/s0022-1694(98)00259-5

Olomu MO, Racz GJ, Cho CM (1973) Effect of flooding on the Eh, pH, and concentrations of Fe and Mn in several Manitoba soils. Soil Sci Soc Am Proc 37:220–224. doi:10.2136/sssaj1973.03615995003700020019x

Patrick WH, Jugsujinda A (1992) Sequential reduction and oxidation of inorganic nitrogen, manganese, and iron in flooded soil. Soil Sci Soc Am J 56:1071–1073. doi:10.2136/sssaj1992.03615995005600040011x

Puget P, Lal R (2005) Soil organic carbon and nitrogen in a Mollisol in central Ohio as affected by tillage and land use. Soil Tillage Res 80:201–213. doi:10.1016/j.still.2004.03.018

R Core Team (2013) R: A language and environment for statistical computing. R foundation for statistical computing, Vienna, Austria. url:http://www.R-project.org/

Roudier P, Manderson A, Hedley C (2016) Advances towards more quantitative assessments of soil profile properties. In: Hartemink AE, Minasny B (eds) Digital soil morphometrics. Springer, Dordrecht

Schaetzl RJ (1998) Lithologic discontinuities in some soils on drumlins: theory, detection, and application. Soil Sci 163:570–590. doi:10.1097/00010694-199807000-00006

Schwen A, Backus J, Yang Y, Wendroth O (2014) Characterizing land use impact on multi-tracer displacement and soil structure. J Hydrol 519:1752–1768. doi:10.1016/j.jhydrol.2014.09.028

Steffens M, Buddenbaum H (2013) Laboratory imaging spectroscopy of a stagnic Luvisol profile—high resolution soil characterisation, classification and mapping of elemental concentrations. Geoderma 195:122–132. doi:10.1016/j.geoderma.2012.11.011

Steffens M, Kohlpaintner M, Buddenbaum H (2014) Fine spatial resolution mapping of soil organic matter quality in a Histosol profile. Eur J Soil Sci 65:827–839. doi:10.1111/ejss.12182

Stolt MH, Baker JC, Simpson TW (1993) Soil-Landscape Relationships in Virginia: I. Soil Variability and Parent Material Uniformity. Soil Sci Soc Am J 57:414–421. doi:10.2136/sssaj1993.03615995005700020022x

Tisdall JM, Oades JM (1982) Organic matter and water-stable aggregates in soils. J Soil Sci 33:141–163. doi:10.1111/j.1365-2389.1982.tb01755.x

Wilkinson M, Richards P, Humphreys G (2009) Breaking ground: pedological, geological, and ecological implications of soil bioturbation. Earth Sci Rev 97:257–272. doi:10.1016/j.earscirev.2009.09.005